# Tunable and Compact SiP Quasi-Dichroic Filter with ≥10 dB/nm Roll-Off Across C- & L-bands

Asher Novick, Songli Wang, Anthony Rizzo, Robert Parsons, Kaylx Jang, and Keren Bergman
Department of Electrical Engineering,
Columbia University, New York, New York, 10027
Email: asn2137@columbia.edu

2022 International Conference on Numerical Simulation of Optoelectronic Devices (NUSOD) | 978-1-6654-7899-1/22/$31.00 ©2022 IEEE | DOI: 10.1109/NUSOD54938.2022.9894746

***Abstract*—We report simulated performance for an integrated and compact silicon photonic quasi-dichroic filter with ≥10 dB/nm roll-off and ≥20 dB extinction ratio between pass and stop bands. Additionally, the cutoff wavelength and compensation for fabrication error are each thermally tunable. The functional dichroic bandwidth is ≈80 nm, which spans most practical use cases.**

## I. Introduction

With the growing interest in on-chip dense wavelength division multiplexing (DWDM) optical interconnects, new silicon photonic (SiP) link architectures have arisen to achieve unprecedented bandwidth densities (5 Tbps/mm$^2$) and energy efficiencies (sub-pico Joule/bit) [1]. Central to many DWDM on-chip architectures is the question of how to utilize the greatest number of WDM channels ($N_{chans}$) at a given data rate per channel ($f_{chan}$). $N_{chans}$ is determined by the total optical bandwidth utilized by the link ($\Delta\lambda_{link}$) divided by the optical channel spacing ($\Delta\lambda_{chan}$).

Typically, the smallest $\Delta\lambda_{chan}$ is calculated based on minimizing the crosstalk penalty between channels, which is strongly dependent on $f_{chan}$ and the resonant filters' quality factor ($Q$). On the other hand, the maximum $\Delta\lambda_{link}$ is limited by the smallest device free spectral range (FSR) present in the architecture. While recent work has demonstrated a Vernier-like scheme to operate ultra-broadband comb-driven DWDM links across a multi-FSR regime [1], such a scheme requires every component in the link to operate near-uniformly across the full $\Delta\lambda_{link}$.

An ideal dichroic filter circumvents this constraint, allowing the spectrum to be split at a specific cutoff wavelength ($\lambda_{co}$). Prior work on integrated true-dichroic filters has been practically limited by large device footprints, poor performance metrics, lack of tunability, and susceptibility to fabrication variation [2], [3]. Yet true-dichroic filters are often unnecessary as DWDM applications will have other factors limiting $\Delta\lambda_{link}$. One solution is to create a quasi-dichroic filter with a ring-assisted Mach Zehnder interferometer (RAMZI), where the functional dichroic bandwidth is twice the assist ring's FSR [4].

Here we show simulations for a RAMZI-based compact and low loss quasi-dichroic filter, with functional dichroic bandwidth covering nearly the full C- & L-bands. Unlike prior designs, the device also allows for thermal tuning to compensate for fabrication variations and fine tune device performance, such as $\lambda_{co}$, post-fabrication.

## II. RAMZI Analytical Model

The expected transmission spectra for each RAMZI output can be calculated analytically using the following equations:

$$L_r = 2\pi r_{ring}, \qquad \Delta L = \frac{L_r}{2} + \frac{\lambda_c}{4n_g}, \qquad \beta = \frac{2\pi n_g}{\lambda}$$

$$A_d = 10^{-\frac{\alpha d}{10}}, \quad B_i = \sqrt{1-k_i}, \quad C_i = \frac{B_i - A_{L_r}e^{j\beta L_r}}{1 - A_{L_r}B_i e^{j\beta L_r}}$$

$$E_{odd} = A_L e^{j\beta L} C_1 C_3, \qquad E_{even} = A_L e^{j\beta L} A_{\Delta L} e^{j\beta \Delta L} C_2$$

$$E_{upper} = \frac{1}{2}\left(E_{odd} - E_{even}\right), \quad E_{lower} = \frac{j}{2}\left(E_{odd} + E_{even}\right)$$

$$T_{upper} = |E_{upper}|^2, \qquad T_{lower} = |E_{lower}|^2$$

Where $r_{ring}$ is the radius of the assist rings, $n_g$ is the group index of the propagating optical mode, $\lambda_c$ is the center wavelength of $\Delta\lambda_{link}$, $L$ is the length of the shorter RAMZI arm (coupled to odd numbered rings), $\Delta L$ is the path length difference between the two RAMZI arms, $\alpha$ is the propagation loss in dB/m, $E_{odd}$ and $E_{even}$ are the respective electric fields of the shorter and longer RAMZI arms, and $T_{upper}$ and $T_{lower}$ are the respective transmission spectra of the upper and lower RAMZI outputs, as shown in Fig. 1a. An example set of transmission spectra derived from the equations above is shown in Fig. 1b.

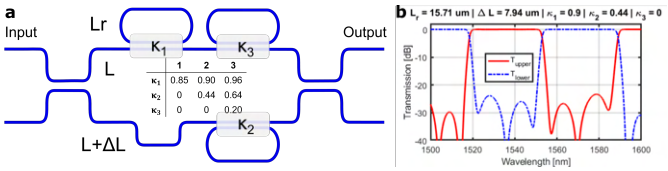


Fig. 1. **a)** Illustration of the analytical model for 3 basic RAMZI configurations, including 1, 2, and 3 assist rings. For each case, $\kappa_i$ is the optical power coupling coefficient into each ring from the respective RAMZI arm, optimizing for flatness in the pass-band [4]. **b)** Analytically modeled output spectra of 2-ring configuration RAMZI with $r_{ring} = 2.5\mu m$ and $n_g = 4.35$. Band suppression ratio is 20+ dB and the functional dichroic bandwidth is 70+ nm. Filter roll-off, measured from the 3 dB point to 20 dB, is 7.8 dB/nm.

## III. Numerical Simulation

The RAMZI assist rings operate in the deeply overcoupled regime ($\kappa_1 \geq 0.85$) and are often in the racetrack style

configuration, with either long straight directional couplers (DCs) or asymmetric 2x2 MMIs coupling between the MZI arms and respective rings. To maximize the functional dichroic bandwidth, a racetrack style ring is not usable, as the increased coupling length contributes to resonator path length, decreasing the FSR. Instead, radial rings with wrap-around style $\kappa$-matched bent directional couplers (BDCs) can be used to achieve the requisite coupling strength, while also taking advantage of the improved broadband performance of BDCs relative to symmetric DCs [5]. While using a BDC to extend the physical coupling length can achieve the requisite coupling over the necessary bandwidth, there still remains a trade-off in device performance and FSR due to increasing bend loss in the assist ring as the radius of curvature decreases [4].

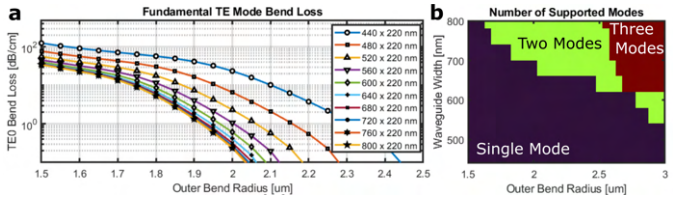


Fig. 2. Results from an FDE solver for a bent SOI slab waveguide with a 220 nm height, varying the waveguide width and bend radius (defined from the bend radial origin to the outer waveguide edge). **a)** $TE_0$ bend loss increases with reduced radius and reduces with increased width due to higher mode confinement. **b)** Tight bends change the single-mode cut off condition, for $r_{bend} = 2.5\mu m$ waveguides as wide as 620 nm remain single-mode.

Finite Difference Eigenmode (FDE) simulations show that, for the fundamental TE mode ($TE_0$) of a 220 nm tall silicon-on-insulator (SOI) slab waveguide, bend loss increases with reduced bend radius, but also decreases as the waveguide gets wider, illustrated in Fig. 2a. Under non-bent conditions, increasing the waveguide width past 500 nm would result in supporting multiple modes, risking parastic inter-mode coupling that degrades performance. As shown in Fig. 2b, tight bends alter the waveguide's single-mode cut off conditions, and a deeply multi-mode straight waveguide may only support a single guided mode if bent tightly enough.

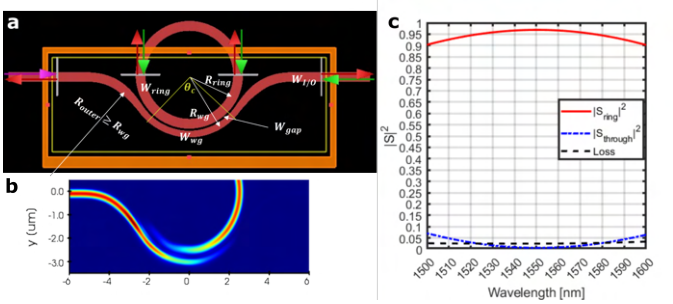


Fig. 3. **a)** Geometrical parameterization in the FDTD solver for a ring resonator with a wrap-around $\kappa$-matched BDC. **b)** Propagation of light through the geometry when $TE_0$ is launched from the left port at $\lambda$ = 1550 nm. **c)** The $|S|^2$ as a function of wavelength optimizing for $\kappa = 0.96$.

Parameterizing the device geometry, shown in Fig. 3a, it is possible to use optimization algorithms in combination with a 3D Finite Difference Time Domain (FDTD) solver to find geometrical configurations that achieve each of the 6 different nominal coupling targets defined in Fig. 1a. Fig. 3a shows the FDTD geometry for the $\kappa_1 = 0.96$ case, Fig. 3b illustrates the power coupling between the bent waveguide and ring for $\lambda = 1550$ nm, and Fig. 3c plots the wavelength dependent power coupling into the ring, leftover power in the waveguide, and excess loss.

The S-parameters solved in FDTD for each ring were exported into Lumerical Interconnect to validate the overall device performance of each configuration, shown in Fig. 4. The simulated functional dichroic bandwidth can exceed 70 nm and reach up to 10 dB/nm roll-off at $\lambda_{co}$.

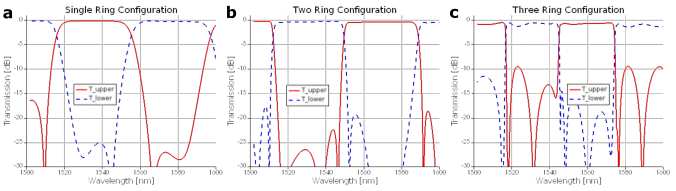


Fig. 4. Simulated device performance for several different RAMZI-based quasi-dichroic filters. In all cases, passband insertion loss is less than 1 dB. **a)** One assist ring, functional dichroic bandwidth is 80+ nm with a roll-off of 2.5 dB/nm at $\lambda_{co}$. **b)** Two assist rings, functional dichroic bandwidth is 75+ nm with a roll-off of 8.5 dB/nm at $\lambda_{co}$. **c)** Three assist rings, functional dichroic bandwidth is 55+ nm with a roll-off of 10 dB/nm at $\lambda_{co}$.

## IV. Discussion & Conclusion

In terms of roll-off, insertion loss, cross-talk and footprint, for a finite $\Delta\lambda_{link}$, RAMZI-based integrated quasi-dichroic filters show improved performance relative to true-dichroic filters [2], [3]. While the functional-dichroic bandwidth of this RAMZI-based filter is fundamentally limited by the ring FSR, simulations clearly demonstrate the feasibility of this approach supporting DWDM architectures with $\Delta\lambda_{link}$ exceeding 70 nm. The RAMZI-based filter is also more compact, has sharper roll-offs, and is less susceptible to small variations in splitting ratios than equivalent MZI-lattice filters. Finally, unique to this approach, a freely tunable $\lambda_{co}$ allows for flexible reconfigurability depending on the application.

## References

[1] A. Rizzo, A. Novick, V. Gopal, and et al, "Integrated kerr frequency comb-driven silicon photonic transmitter," 2021. [Online]. Available: https://arxiv.org/abs/2109.10297

[2] E. S. Magden and et al, "Transmissive silicon photonic dichroic filters with spectrally selective waveguides," *Nature Communications*, vol. 9, no. 1, 2018.

[3] A. Y. Piggott and et al, "Inverse design and demonstration of a compact and broadband on-chip wavelength demultiplexer," *Nature Photonics*, vol. 9, no. 6, p. 374–377, 2015.

[4] L.-W. Luo and et al, "High bandwidth on-chip silicon photonic interleaver," *Opt. Express*, vol. 18, no. 22, pp. 23 079–23 087, Oct 2010.

[5] H. Morino and et al, "Reduction of wavelength dependence of coupling characteristics using si optical waveguide curved directional coupler," *J. Lightwave Technol.*, vol. 32, no. 12, pp. 2188–2192, Jun 2014.